C. R. Physique 11 (2010) 18–29

Contents lists available at ScienceDirect

Comptes Rendus Physique

www.sciencedirect.com

Propagation and remote sensing / Propagation et télédétection

Assessment of rain fade mitigation techniques in the EHF band on a Syracuse 3 20/44-GHz low elevation link

Prédiction des techniques de mitigation de l'affaiblissement en bande EHF dans le cadre du programme Syracuse 3 20/44 GHz

L. de Montera [a,*], L. Barthès [a], C. Mallet [a], P. Golé [a], T. Marsault [b]

[a] *Université Versailles Saint-Quentin en Yvelines (UVSQ), laboratoire atmosphères, milieux, observations spatiales (LATMOS), 10-12, avenue de l'Europe, 78140 Vélizy-Villacoublay, France*
[b] *Centre d'électronique de l'armement (CELAR), Bruz, France*

ARTICLE INFO

Article history:
Available online 21 February 2010

Keywords:
Propagation
Attenuation
Rain fade
Mitigation
Frequency scaling
EHF band

Mots-clés :
Propagation
Affaiblissement
Prédiction
Précipitation
Transposition en fréquence
Bande EHF

ABSTRACT

An Earth-to-satellite propagation experiment in the EHF band has been carried out within the framework of the Syracuse 3 program, which is a new generation French military SATCOM system. The originality of this experiment resides in the link's frequencies (20 GHz downlink and 44 GHz uplink) and its low elevation angle (17°). The first part of the article presents a statistical analysis of attenuation data providing the long-term statistics, frequency scaling ratios and fade durations. These results are compared to standard ITU models. The second part of the article is dedicated to the short-term forecasting of rain fade, useful for the implementation of Fade Mitigation Techniques (FMT). Firstly, the downlink attenuation is predicted based on a non-linear ARIMA-GARCH model. The prediction result is then separated into several physical components (gases, clouds and rain) that are scaled to the uplink frequency using specific frequency scaling factors. The performance of the model is assessed based on Syracuse 3 20/44-GHz data collected during a period of 1 year.

RÉSUMÉ

Une expérience de propagation Terre–Satellite en bande EHF a été réalisée dans le cadre du programme Syracuse 3 qui est la nouvelle génération de satellites militaires français de télécommunication. L'originalité de cette expérience réside dans les fréquences utilisées (20 GHz pour la liaison descendante et 44 GHz pour la liaison montante) et dans le faible angle d'élévation (17°). La première partie de l'article présente une analyse statistique des données concernant notamment les probabilités de dépassement, les coefficients de transposition en fréquence et les durées d'affaiblissement. Ces résultats sont comparés aux modèles standards de l'UIT. La seconde partie de l'article est dédiée à la prédiction à court-terme de l'affaiblissement qui est une étape généralement nécessaire pour implémenter des techniques adaptatives de lutte contre l'affaiblissement (FMT). L'affaiblissement sur la liaison descendante est tout d'abord prédit à l'aide d'un modèle ARIMA-GARCH non-linéaire. La prédiction est ensuite séparée en plusieurs composantes physiques (gaz, nuages et pluie) qui sont transposées à la fréquence de la liaison montante par des coefficients

* Corresponding author.
E-mail address: louis.demontera@latmos.ipsl.fr (L. de Montera).

1631-0705/$ – see front matter
doi:10.1016/j.crhy.2009.12.002

de transposition spécifiques. Les performances du modèle sont évaluées avec des données Syracuse 3 collectées pendant une période d'un an.

1. Introduction

The ever-increasing demand for capacity in communication channels has led the SATCOM industry to develop new satellite systems operating at frequencies above 20 GHz where large bandwidths are available (EHF band – Extremely High Frequencies). Nevertheless, the attenuation effects of atmospheric gases, clouds and rain can reach significant levels at these frequencies and it is no longer cost-effective to use a fixed power margin. Rain attenuation, due to scattering and absorption by water droplets, is the major limitation for satellite links in the EHF band. Since rain events have a limited extension in time and space, various adaptive Fade Mitigation Techniques (FMT) have been developed to make communications at these frequencies possible. Whatever the FMT used, short-term forecasting of rain attenuation is necessary to track the propagation channel variations and trigger power compensation only when needed.

In order to increase knowledge on propagation in the EHF band and in preparation for future military telecommunication systems, the French Délegation générale de l'armement (DGA) has decided to equip its third generation of operational telecommunication satellites with 20/44-GHz systems. An EHF propagation experiment has been set up and two years of data have been collected at a low elevation angle of 17°. The experiment and pre-processing of the data are detailed in Section 2. Since data currently available for this type of configuration is scarce, the Syracuse 3 experiment was a good opportunity to test the accuracy of International Telecommunication Union (ITU) models and to assess that of short-term forecasting models.

A number of statistical analyses are presented in Section 3. Yearly and monthly cumulative attenuations at 20 and 44 GHz were computed and compared with those predicted by the corresponding ITU model. A statistical analysis of instantaneous frequency scaling coefficients is then presented. Frequency scaling is often required for FMT in order to predict uplink behavior from the downlink, which generally operates at a lower frequency. Experimental frequency scaling ratios obtained between 20 and 44 GHz were compared with those given by existing ITU models and the influence of gases and clouds was investigated. Furthermore, fade duration statistics were then determined. A moving average window was used to filter out scintillation in the measured signal, and the influence of its size is discussed. Finally, fade durations computed under different filtering conditions were compared with the standard ITU model and the Cheffena–Amaya model [1], which is based on unfiltered data.

The problem of rain fade short-term forecasting is addressed in Section 4. Typically, the required forecast interval ranges between 2 and 60 seconds, which corresponds to the control loop reaction time. Unfortunately, even over such short time intervals, rain attenuation behaves similarly to a random walk, with very small autocorrelation. In order to overcome this difficulty and for better prediction performance, stochastic models originally developed for financial applications have been adapted to this problem. Indeed, rain fade and financial assets time series have similar second-order statistics: both exhibit a clustering of highly volatile periods ('heteroscedasticity') and fat tailed distributions of variations ('leptokurticity'). In a previous paper based on the 20-GHz Olympus beacon data, we had shown that rain fade time series could be modeled by a switching ARIMA process (Auto Regressive Integrated Moving Average) with non-linear GARCH errors (Generalized Auto Regressive Conditionally Heteroscedastic) [2]. The originality of this model is that it allows one to predict not only the attenuation level, but also the error conditional distribution, thus providing an accurate upper bound for future attenuation. This new model has already been tested against a subset of the 20-GHz Syracuse 3 attenuation database, and has been shown to significantly outperform other existing models in terms of link availability [3]. In this paper, the parameters of the ARIMA-GARCH model are estimated based on a one-year data set, in combination with a frequency scaling model used to predict the uplink attenuation from the downlink measurements. The prediction model using frequency scaling from 20 to 44 GHz has been simulated over a whole year of available data. Its performance is illustrated for different forecast intervals and compared with a simple prediction persistence-based model.

2. Experimental set-up

Syracuse is a French military program for secure Earth–satellite telecommunications developed since the beginning of the 1980s by the DGA. The first satellite of its third generation, Syracuse 3A, was launched in October 2005. This satellite has been placed on a geostationary orbit at 47° E vertically above Kenya. It carries a conventional communications system in the SHF band (Super High Frequency), another communications system in the EHF band, and a positioning beacon at 20 GHz. The SHF system operates at 7–8 GHz and includes four spot beams and nine 40 MHz bandwidth channels. The EHF system operates at 20–44 GHz and includes two spot beams and six 40-MHz bandwidth channels. The whole French metropolitan territory is covered by the EHF system. 44-GHz uplink signals are received by onboard repeaters which amplify and retransmit the signals to Earth stations on the 20-GHz downlink. This configuration has been designed in order to minimize the satellite's power consumption. In particular, since the 44-GHz link is more affected by atmospheric attenuation, its transmission requires more power. The measurement of the 20-GHz downlink is performed directly on the signal received from the satellite beacon. As to the 44-GHz uplink, the measurement is not straightforward: the received power depends on the sum of the uplink and downlink attenuations, since the signal is repeated by the satellite. Therefore, the 44-GHz

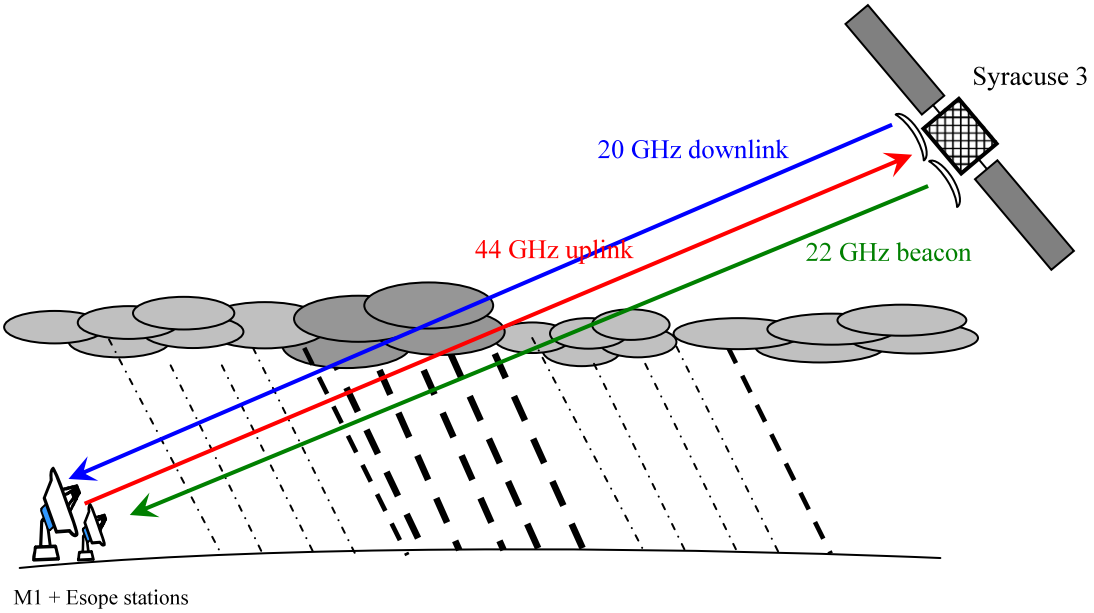

Fig. 1. Experimental set-up (CELAR site only).

received power is estimated by subtracting the 20-GHz received power measured on the satellite beacon from the total received power (Fig. 1). Note that the power transmitted by the Earth stations was adjusted so that the onboard repeaters remain linear under all meteorological conditions.

The experimental set-up involves several Earth stations [3]. However, in this study, only the signal transmitted by an operational station (the M1 station) located at the CELAR site in Rennes, France, was considered. Since operational systems usually do not allow sufficiently accurate measurements to be performed, it was decided to receive the signal using an experimental station located at the same location and specifically designed for research applications (the ESOPE station). This receiver system had been previously developed in the framework of the STENTOR propagation experiment, which had been cancelled due to the failure of its Ariane launcher in 2003. The experimental set-up is furthermore advantageously combined with a Dual-Beam Spectropluviometer (DBS) [4] and a multi-frequency radiometer pointing towards the satellite. The antenna is also protected from rain by means of an awning and a blower. Moreover, the measurements are sampled at 100 Hz and averaged over 1 s periods to reduce scintillation noise with respect to that of conventional measurement systems such as spectrum analyzers.

In practice, the Earth station only measures a received power because the satellite's transmission power is not known exactly. The 0-dB attenuation reference level must therefore be estimated. This level is provided by the radiometer, which measures the sky brightness temperatures at two frequencies that are sensitive to water vapor and cloud water, thus providing a very accurate estimation of atmospheric attenuation during clear sky periods [5] (by means of a neural network-based model [6]). It is also necessary to separate atmospheric attenuation from power variations due to instrumental instabilities. Normally, these instrumental offsets can be estimated as the difference between the radiometric clear sky attenuation and the received power. This is usually computed as a 24-hour long time series, called a *template*, which is then smoothed and interpolated during rainy periods in which the radiometer-estimated attenuation is unreliable because of saturation. The *template* is then subtracted from the received power in order to retrieve the actual atmospheric attenuation of the transmitted signals. Because of the positional variations of the satellite (which is seen from the Earth as moving along a '∞' shaped trajectory) caused by Earth's non-perfectly spherical shape, the *template* is generally a sinusoid with a period of 24 h. The amplitude of this periodic variation is 2–3 dB at 44 GHz. The variations of the template can also be due to temperature variations affecting the satellite's power supply or periodic repositioning of the satellite to correct its departure from geostationary orbit.

3. Statistical analysis

3.1. Attenuation statistics

Figs. 2 and 3 show the excess probabilities of 20-GHz and 44-GHz attenuations, respectively, derived from the measurements performed at CELAR in 2007 and 2008. The excess probability is defined as a function of the attenuation level, as the time percentage during which the latter is exceeded. Data availability was 75% for both the 20-GHz and 44-GHz channels in 2007 and 74% and 70%, respectively, in 2008. Note that long-term statistics are not biased by this limited availability because

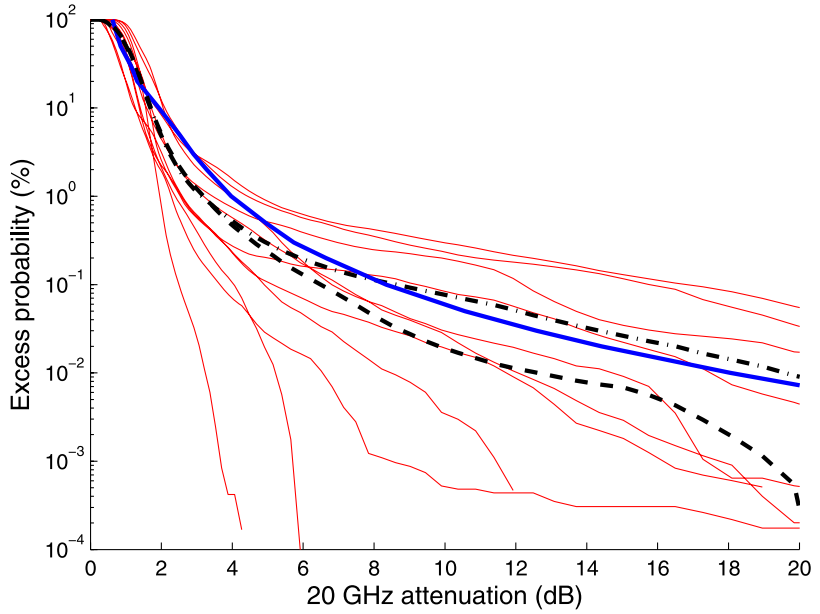

Fig. 2. 20-GHz total attenuation cumulative distribution computed on 2007 data (dash–dot curve) and 2008 data (dashed curve) compared with the standard ITU model (solid line). Thin curves correspond to monthly statistics obtained in 2007.

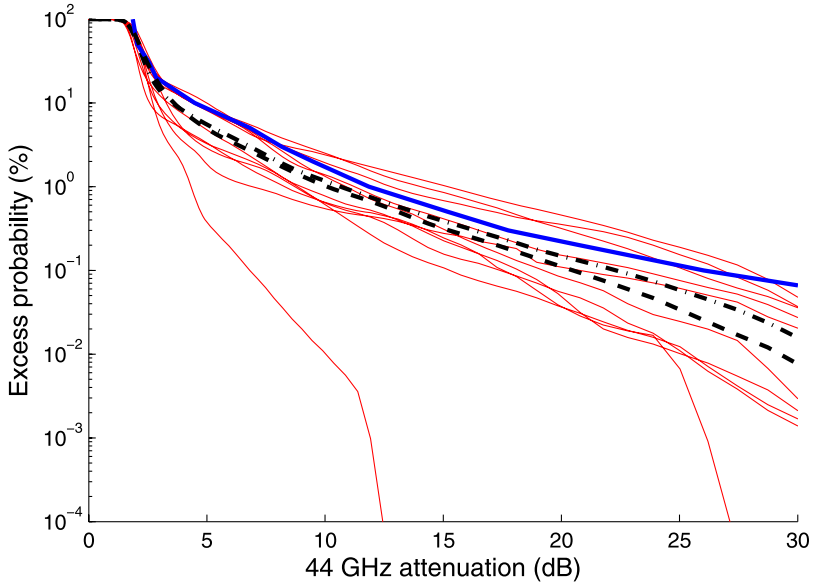

Fig. 3. 44-GHz total attenuation cumulative distribution computed on 2007 data (dash–dot curve) and 2008 data (dashed curve) compared with the standard ITU model (solid line). Thin curves correspond to monthly statistics obtained in 2007.

it is mainly due to breakdowns of the radiometer that are uncorrelated with the meteorological situation. The statistics obtained from the 20-GHz attenuation measurements (Fig. 3) are consistent with the prediction provided by the ITU models combined in order to obtain the excess probability of total attenuations [7], within the interannual variability (compare the dashed black curve with the solid black curve for 2007 and 2008, respectively). Fig. 4 shows that the same consistency with ITU model predictions can be observed for the 44-GHz statistics. Note that unfortunately, in 2007, the radome of the 44-GHz transmitting antenna had not yet been provided with the awning protection against droplets remaining after each rain event, thus causing an overestimation of up to 3 dB of atmospheric attenuation at this frequency during and immediately after each rain event, which only slowly decreased afterwards as the droplets evaporated from the radome. This problem has been addressed in [3]. A blower was finally mounted on the antenna so as to remove these droplets, and as a result, the 2008 statistics have not been affected. In both Figs. 2 and 3, the red curves show the monthly attenuation statistics and

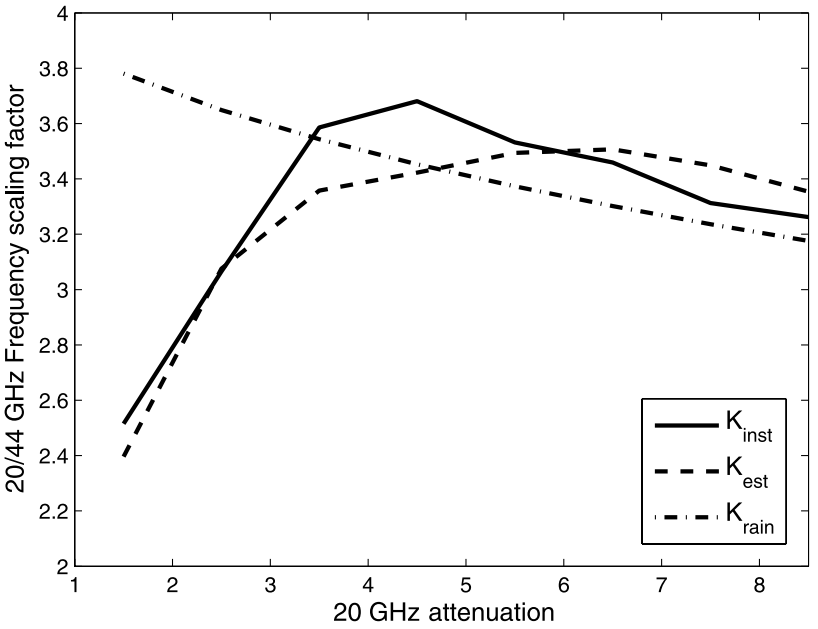

Fig. 4. Mean 20/44-GHz frequency scaling factor as a function of 20-GHz attenuation. K_{inst} is the instantaneous scaling factor (solid curve), K_{est} is the scaling factor estimated by separating physical effects (dashed curve), and K_{rain} is the scaling factor given by the ITU model for rain attenuation (dash–dot curve).

illustrate the high variability of attenuation statistics. (For interpretation of the colors in these figures, the reader is referred to the web version of this article.)

3.2. Frequency scaling from Ka to Q band

The instantaneous frequency scaling ratio, denoted K_{inst}, represents the relationship between simultaneous attenuations at different frequencies, f_1 and f_2,

$$K_{inst}(t) = \frac{A_{f_2}(t)}{A_{f_1}(t)} \tag{1}$$

where $A_f(t)$ denotes attenuation at frequency f in GHz and at time t. In the framework of FMTs, this ratio must be estimated in order to predict the uplink attenuation from the downlink signal, which is generally at a lower frequency (f_2 and f_1 in Eq. (1) denote the uplink and downlink frequencies, respectively). This is usually done by means of ITU models which are specific to rain attenuation. However, above 20 GHz, the effect of the atmospheric gases and clouds cannot be neglected (their combined effect may reach as much as 6–8 dB attenuation at 44 GHz and at a 17° elevation angle). Therefore a separation of these physical effects must be performed because the various atmospheric contributions (rain, gases and clouds) behave differently as a function of frequency, thus requiring a different frequency scaling ratio for each of these effects. A neural network had previously been developed for this purpose [6]. The input data is the 20-GHz attenuation, together with ground meteorological data, which have been shown to improve the performance of the neural network (pressure, temperature and humidity). The output of the neural network provides an estimation of the normalized weights of each contribution to the overall measured attenuation (denoted W_{gas}, W_{clouds} and W_{rain}). Once the separation of these three effects has been carried out, frequency scaling can be performed. The estimated scaling factor, denoted K_{est}, can be written as follows, using the normalized weights:

$$K_{est} = W_{gas}.K_{gas} + W_{clouds}.K_{clouds} + W_{rain}.K_{rain} \tag{2}$$

where K_{gas}, K_{clouds} and K_{rain} are the specific scaling factors of each contribution estimated from standard ITU models (cf. [7–9]). In the case of a 20–44-GHz link, K_{clouds} is equal to 4.5 while K_{gas} and K_{rain} range from 1.5 to 2 and from 3 to 3.8, respectively, depending on humidity for the former and on the attenuation level for the latter.

Fig. 4 shows a comparison between the experimental frequency scaling ratio (K_{inst}, solid curve) and the one estimated based on the model described above (K_{est}, dashed curve). These instantaneous frequency scaling ratios have been averaged over 20-GHz attenuation intervals and plotted as functions of this attenuation. For small attenuations, gases contribute most, and the instantaneous frequency scaling ratio is approximately 2.5. K_{est} was found to be in good agreement with this value. It should be noted that using K_{rain} (dash–dot curve) instead of K_{inst}, would result in an overestimated ratio because of the small contribution of rain. For larger attenuations, K_{inst} increases with the contribution of clouds and reaches a maximum of

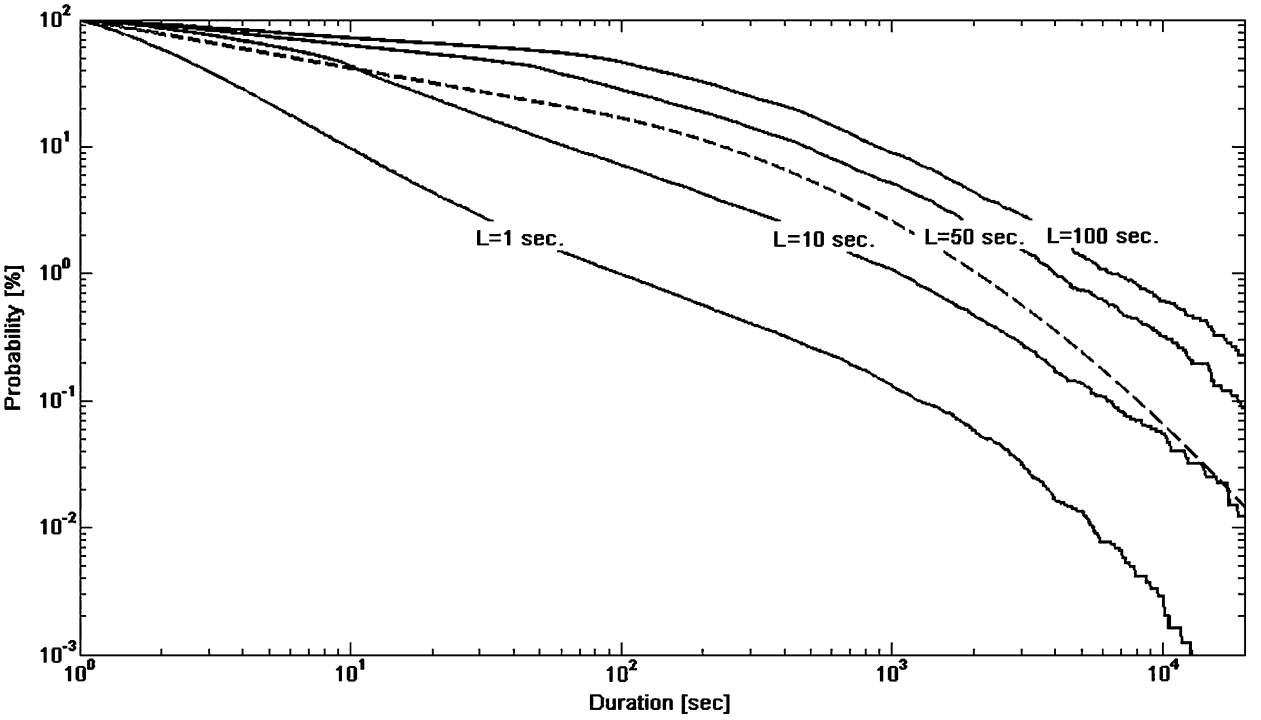

Fig. 5. Cumulative fade duration distributions obtained at 20 GHz for different filter lengths ($L = 1$, 10, 50 and 100 seconds) (solid lines) and the ITU1623 model (dashed line), with $A = 2$ dB.

3.65 for an attenuation of 4.5 dB at 20 GHz. Beyond this value, rain contributes increasingly to the overall attenuation and K_{inst} logically tends to the frequency scaling ratio of the rain contribution alone. However, the specific frequency scaling factor of rain contribution is very similar to K_{inst} only at high attenuation levels, thus underlining the fact that such a simplified model is not adequate in the context of the EHF band. On the other hand, the frequency scaling ratio estimated by separating the physical effects is in better agreement with K_{inst} whatever the attenuation level.

3.3. Fade duration

Fade durations were extracted from Syracuse 3 measurements at 20 GHz. The cumulative distribution is the probability of occurrence of fades with a duration d longer than D for an attenuation a greater than a fixed threshold A, i.e. $\Pr[d > D \mid a > A]$. Fade duration statistics depend on link configuration (frequency, location and elevation angle) and on the preprocessing method. For our purpose, the data were low-pass filtered by a moving average method with four different window sizes, of $L = 1$, 10, 50 and 100 seconds. Fig. 5 shows the cumulative fade duration distributions for the period from February 2007 to December 2008 with a threshold of $A = 2$ dB. The solid lines were obtained using the different filters and the dashed curve shows the ITU1623 model [10]. As described in the ITU recommendations, the obtained curves can be divided into two parts. Shorter fade durations can be described by a power law whereas longer fade durations are better represented by a log-normal law. In addition, as observed in Fig. 5, the cumulative distributions depend on the length L of the filter. The typical filter length $L = 50$ seconds (0.02-Hz cut-off frequency) is often used to remove scintillation. Unfortunately, this filter tends to artificially increase the durations of events shorter than L and therefore decreases their occurrences. As a consequence, the slope of the cumulative distributions decreases as L increases. It can be seen from Fig. 5 that this effect is restricted to durations shorter than the filter length for which each curve has its own slope. As expected, for durations longer than the filter length, the filter does not affect the statistics and the slopes remain similar. Thus, in our opinion, unfiltered data (more specifically 1-second filtered data) should be used to estimate fade durations in order to avoid the artificial and unnecessary effect of filtering.

Fig. 6 compares the empirical cumulative distributions computed with unfiltered data to ITU1623 and Cheffena–Amaya models [1] for four different thresholds ($A = 2$, 4, 8 and 10 dB). It may be seen that for all thresholds, the left part of the curves is well represented by a simple power law, in agreement with ITU1623. This power law is valid from 1 second to about 30 min or 1 hour, depending on the threshold. The main difference between empirical cumulative distributions and ITU1623 is that the slope is threshold-dependant while the sensitivity to the threshold is very small for ITU1623. Although the Cheffena–Amaya model uses a log-normal function to represent the left part of the cumulative distributions instead of the power law observed in Fig. 6, it fits our data better than the ITU model. This conclusion is confirmed by the likelihood calculation, which gives greater values for the Cheffena–Amaya model.

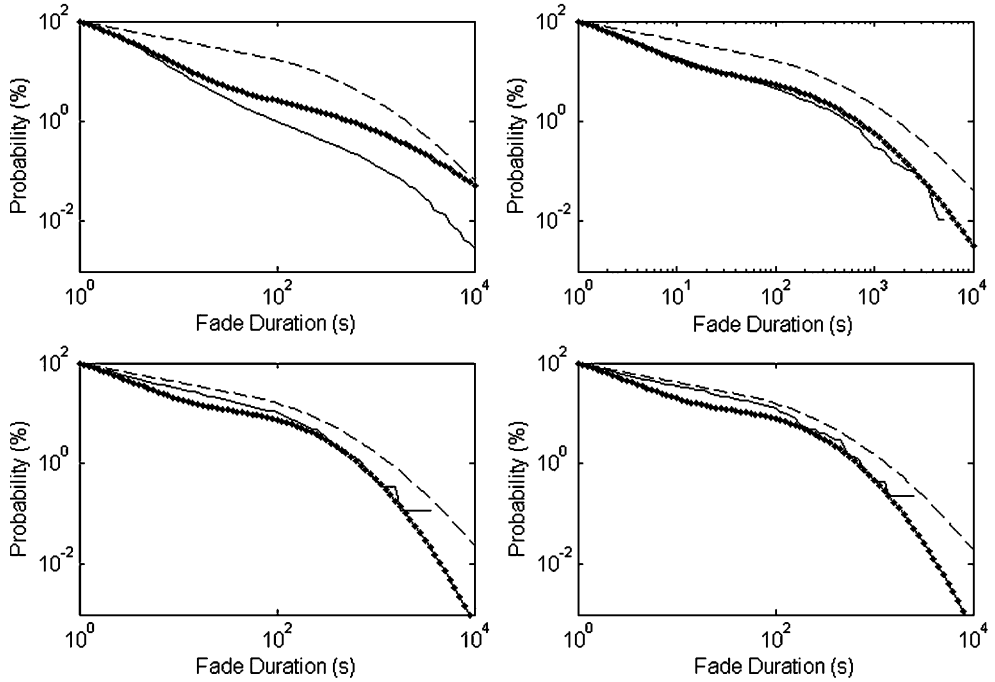

Fig. 6. Cumulative fade duration distributions obtained at 20 GHz for different attenuation levels (from left to right and top to bottom, $A = 2$, 4, 8 and 10 dB) with $L = 1$ second (solid curve) compared with the ITU1623 model (dashed curve) and the Cheffena–Amaya model (solid–dot line).

4. Rain fade forecasting

4.1. Syracuse 3 20/44-GHz data

A database was created from 20-GHz and 44-GHz attenuations sampled at 1 Hz measured at the CELAR site in Rennes, France, in 2007 and 2008. Since the stochastic rain fade prediction models presented in this paper were developed for real-time applications, the data were unfiltered. Moreover, only periods of valid data were considered. Data collected in 2007 were used to estimate the parameters of the prediction models. This part of the database comprises at least 144 h of rain (the criteria being that the 20-GHz attenuation exceeds 2.5 dB). The second part of the database comprises at least 161 h of rain and corresponds to measurements performed in 2008. It has been used to assess the performance of the various models. For the prediction model using frequency scaling and involving the 44-GHz measurements, the database used to assess the performance comprises fewer strong rain events because the 44-GHz channel reaches saturation (its maximum measurable attenuation) more often than the 20-GHz channel. Since the instruments cannot measure attenuation above 35 dB and since the 20- to 44-GHz frequency scaling factor is approximately 3.7, only a 20-GHz attenuation smaller than 9 dB could be considered for this purpose.

4.2. The ARIMA-GARCH prediction model

In this section the performance of a short-term prediction model of rain fade which includes frequency scaling from 20 to 44 GHz is presented. The model had been developed previously [2] based on 20-GHz attenuation measurements obtained during the Olympus propagation experiment [11,12]. The analysis of the experimental attenuation time series showed that simple linear stochastic models do not predict the rain fade process accurately because its autocorrelation is nearly zero, even for short time intervals of a few seconds. However, since the aim of fade mitigation techniques is to avoid link outage rather than predicting rain fade level, the present model will estimate an upper bound for the future attenuation that will not be exceeded during a given time percentage. For that purpose, the second-order statistical properties of attenuation time series were investigated. It was found that periods with large attenuation variations were localized in time, that the distribution of the increments was fat-tailed and that the variance of the process had significant autocorrelation. These properties, which are typical of turbulent processes, could indeed be expected since raindrops can be considered as passive scalars advected by atmospheric eddies from the storm scale down to 1 m scales [13]. At this stage, an analogy with the field of finance comes to mind because financial assets generally exhibit a very similar statistical behavior and a major preoccupation of traders is also to estimate risks (or *volatility*) and therefore upper bounds. We therefore sought to adapt a conventional model originally developed for financial applications and to describe rain fade as being a switching ARIMA process (Auto Regressive Integrated Moving Average) with non-linear GARCH (Generalized Auto Regressive Conditionally

Heteroscedastic) errors. The fundamental assumption of this model is that the residuals of the ARIMA model follow a centred Gaussian probabilistic law with a time-varying standard deviation. This conditional variance (or *instantaneous volatility*) is predicted based on its past values combined with the square of the ARIMA residuals. In the following, the basic equations of the prediction model are recalled and the parameters estimated from the Syracuse 3 20/44-GHz data are given (for details about the identification and estimation of the prediction model and for the multi-step algorithm used to implement it, see [2]).

First, a threshold T of 2.5 dB is used to separate fade periods of different physical origins. The periods in which the process is below T are associated with smooth variations and mainly correspond to clear sky or cloud attenuation. The periods in which the attenuation is above T correspond to strong rain events and are expected to be highly *volatile*. The value of the threshold was found using the neural network introduced in Section 3.2, which provides the normalized weights of the different physical effects. It is the level for which, statistically, 50% of attenuation is due to rain. The second step of the model is to achieve stationarity by performing a differentiation, since the process would otherwise be non-stationary and no stable statistical properties could be derived from the analysis. The differentiated time series is denoted $\Delta A_t = A_t - A_{t-1}$ in the following.

The differentiated time series is then modeled as a conventional linear ARMA process in order to make the most of the (limited) information contained in the autocorrelation of the increments. An identification of the orders of the ARMA model yielded the following equation:

$$\Delta\hat{A}_t = \varphi_1 \Delta A_{t-1} + \varphi_2 \Delta A_{t-2} + \theta_1 \varepsilon_{t-1} + \theta_2 \varepsilon_{t-2} \tag{3}$$

where $\Delta\hat{A}_t$ is the predicted differentiated attenuation 1 s forward and $\varepsilon_{t-k} = \Delta A_{t-k} - \Delta\hat{A}_{t-k}$ is the error of the model at time $t-k$. The parameters of the ARMA model are denoted φ'_1, φ'_2, θ'_1, θ'_2 when $A_t \geqslant T$, and φ''_1, φ''_2, θ''_1, θ''_2 when $A_t < T$. The following parameters were found from the Syracuse 3 20/44-GHz data:

$$\begin{pmatrix} \varphi'_1 = 1.2473 \\ \varphi'_2 = -0.3143 \\ \theta'_1 = -1.6809 \\ \theta'_2 = 0.7149 \end{pmatrix} \quad \text{and} \quad \begin{pmatrix} \varphi''_1 = 0.1428 \\ \varphi''_2 = 0.0549 \\ \theta''_1 = -0.6404 \\ \theta''_2 = -0.2984 \end{pmatrix} \tag{4}$$

Since the conditional variance of the ARIMA model residuals is not constant, a non-linear GARCH error model is used in order to derive an adaptive estimation of the confidence intervals related to the predictions. The assumption of Gaussian residuals is expressed by:

$$\varepsilon_t = \eta_t . \sigma_t \tag{5}$$

where σ_t is the conditional standard deviation of the ARMA residuals and η_t is the normalized residual. The model has been validated by the fact that η_t was indeed found to be a Gaussian white noise with a variance of 1 (for a detailed analysis, see [3]). The conditional variance is predicted by a linear combination of its past values and the realized variance, i.e. the square of the current error. The identification led to:

$$\sigma_t^2 = \omega + \alpha . \varepsilon_{t-1}^2 + \beta . \sigma_{t-1}^2 \tag{6}$$

The parameters of the GARCH models are denoted ω', α', β' when $A_t \geqslant T$ and ω'', α'', β'' when $A_t < T$. The following parameters were found based on the Syracuse 3 20/44-GHz data:

$$\begin{pmatrix} \omega' = 2.5\text{e}{-4} \\ \alpha' = 0.0259 \\ \beta' = 0.9719 \end{pmatrix} \quad \text{and} \quad \begin{pmatrix} \omega'' = 2\text{e}{-5} \\ \alpha'' = 0.0413 \\ \beta'' = 0.9554 \end{pmatrix} \tag{7}$$

It is remarkable that these parameters, as well as those of the ARMA models, are very close to those estimated previously using the attenuations of the 20-GHz beacon of the Olympus satellite presented in [2]. (Note that, in the case $A_t < T$, we found an ARMA(2, 2) whereas an ARMA(1, 2) was proposed in [2]. However this difference is not significant since the added parameter φ''_2 is very small.) This shows that the ARIMA-GARCH model is not specific to any given link and, moreover, that its parameters are not strongly sensitive to link geometry, in particular the elevation angle (the Olympus satellite was at an elevation angle of 30° whereas it was only 17° for Syracuse 3).

The next step of the method is to combine and iterate Eqs. (3) and (6) in order to predict the attenuation level, denoted $\hat{A}_{t+k}$, k steps ahead, and its error conditional variance, denoted $\hat{V}_{t+k}$ (this multi-step algorithm is fully described in [2]). The predicted upper bound of the attenuation, denoted $\bar{A}_{t+k}$, is then calculated as follows:

$$\bar{A}_{t+k}(P) = \hat{A}_{t+k} + \bar{M}_{t+k}(P, \hat{V}_{t+k}) \tag{8}$$

where $\bar{M}_{t+k}$ is the adaptive error margin, which depends on the required link availability P. It is conventionally defined as the percentage of time during which the measured attenuation level does not exceed the predicted upper bound. Since the

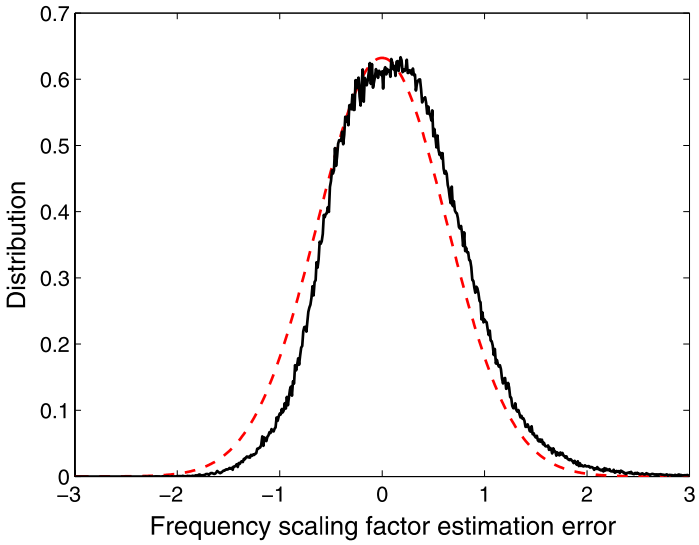

Fig. 7. Distribution of the 20/44-GHz frequency scaling factor estimation error (solid curve) compared with a Gaussian distribution having the same variance (dashed curve).

error is Gaussian, the error margin needed to reach a given availability P can be computed using the Gauss error function erf(.):

$$\bar{M}_{t+k}(P, \hat{V}_{t+k}) = \text{erf}^{-1}\left(\frac{2P}{100} - 1\right)\sqrt{2\hat{V}_{t+k}} \tag{9}$$

As to forecasting the uplink attenuation, the predicted upper bound of the downlink attenuation cannot be scaled directly to Q-band with the method described in Section 3.2 because frequency scaling introduces an additional error which may be too large. In particular, various sources of uncertainty must be taken into account such as the variability of the Drop Size Distribution (DSD), the fact that separating the atmospheric effects is an approximation with its own uncertainties, and that estimating atmospheric profiles from ground meteorological measurements may not reflect the exact reality. As a first approximation, the frequency scaling factor estimation error is found to have a Gaussian distribution with a standard deviation of 0.65 (Fig. 7). Since the prediction error of the ARIMA-GARCH model is also Gaussian (although it has a time-varying conditional variance), it can appropriately be combined with the error due to frequency scaling (see [2]). Finally, the ARIMA-GARCH prediction model with frequency scaling allows an accurate upper bound of forthcoming uplink attenuation to be obtained in real time from the downlink attenuation which will not be exceeded during the required percentage of time.

4.3. Performance of the model

The performance of the ARIMA-GARCH model was compared with that of other existing models based on all available rain periods collected in 2007 and 2008 (rain is assumed to be present when the 20-GHz attenuation exceeds 2.5 dB). A model referred to as persistence is used as the reference and consists in assuming that the process remains constant over the forecast interval and adding a fixed error margin. The other models considered here are the 'two-Sample' model [14–16], the NASA model [17,18] and the ADALINE model [19]. Another model worth of interest is the adaptive ARMA [20], although it was found to be unstable and could not be run over one-year periods. The forecast interval is set to 10 s because this value is typical of the delay of FMT control loops and because some of the investigated models have been specifically designed for this interval (especially the 'two-sample' model). The comparison criterion (called the mean cost and denoted C) is defined, in dB, as the mean overestimation of the attenuation level by the predicted upper bound necessary to avoid link outage during at least P% of the time:

$$C(P) = \frac{1}{N}\sum_{t=1}^{N} H\big(\bar{A}_t(P) - A_t\big)\big(\bar{A}_t(P) - A_t\big) \tag{10}$$

where N is the duration of the attenuation time series in s, and $H(.)$ the Heaviside step function. Since comparing model performance is not relevant during clear sky periods, the results were computed only for strong rain periods ($A_t > T$), which were found to occur for 11% of the time according to Fig. 2. The ARIMA-GARCH model is shown to outperform significantly other existing models (see Fig. 8), thus confirming the previous results obtained based on the Olympus 20-GHz attenuations [2] and on a limited database of Syracuse 3 20-GHz attenuation events [3]. Moreover, note that, as could

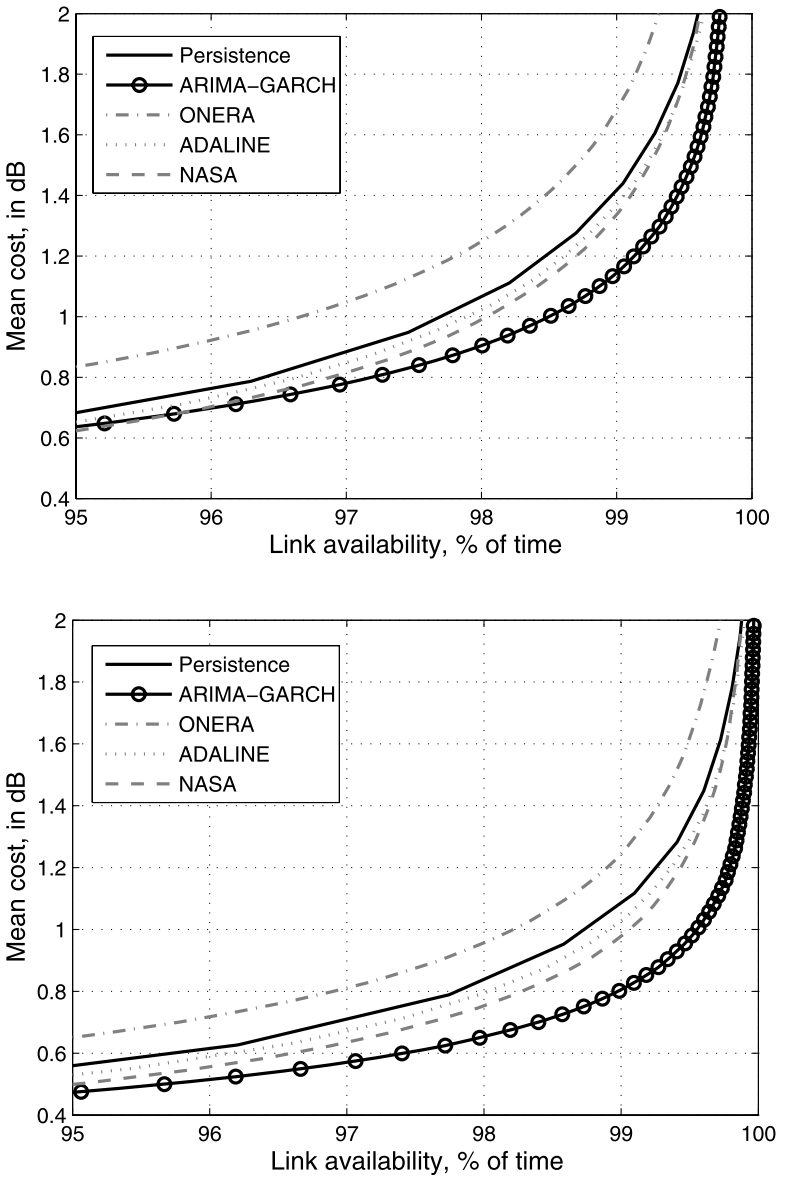

Fig. 8. Cost/availability performance of the prediction models computed from the 20-GHz Syracuse 3 data collected in 2007 (top) and 2008 (bottom) (only the rain periods are considered, i.e. time intervals during which attenuation exceeds 2.5 dB).

be expected, the link availability which is obtained *a posteriori* corresponds closely to the one that was asked *a priori* and denoted P in Eq. (9) (the difference is limited to $\pm 0.2\%$ if the test is performed on one-month time series with $P = 99\%$).

The ARIMA-GARCH model is then combined with the frequency scaling method, which involves separating physical effects (i.e. K_{est}) in order to predict the uplink 44-GHz attenuation. Since no other prediction model involving frequency scaling was reported in the literature, this model could only be compared with simpler ones: the ARIMA-GARCH model, which uses standard ITU frequency scaling (i.e. K_{rain}), and a simple persistence prediction model, which also uses standard ITU frequency scaling. The results given by these increasingly sovarphisticated models are shown in Fig. 9 for different forecast intervals and are computed based on all of the available 44-GHz attenuation data collected in 2008. As can be seen that the ARIMA-GARCH prediction model and the method based on the separation of physical effects both significantly increase performance and must be resorted to if a link availability as high as about 99.9% is desired. It should be noted that the estimation of the frequency scaling factors was found to degrade in real time due to scintillations, so that it was necessary to apply a slightly causal filtering with a moving average window of 10 seconds before performing the estimation.

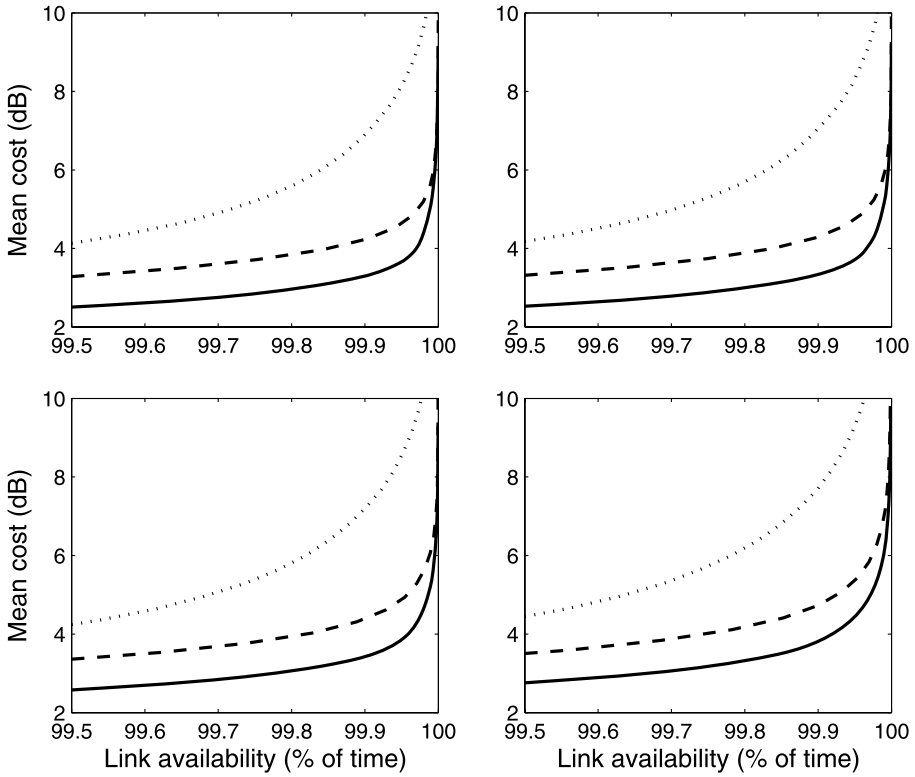

Fig. 9. Cost/availability performance of ARIMA-GARCH with frequency scaling based on the separation of physical effects (solid curve) compared with ARIMA-GARCH using standard ITU frequency scaling (dashed curve) and with a simple persistence prediction model using standard ITU frequency scaling (dotted curve). The performance is computed for all available 44-GHz attenuation data collected in 2008 and for various forecast intervals (from left to right and top to bottom: 5, 10, 15 and 30 seconds).

In order to determine which part of the prediction system contributes most to the uplink prediction error, the contributions of the ARIMA-GARCH prediction error and of the frequency scaling factor error were estimated separately (for rigorous definitions, see [2]). Fig. 10 shows that the contribution of frequency scaling is larger than that of the ARIMA-GARCH method at any forecast interval and that this difference increases with attenuation.

5. Conclusion

Attenuation data has been collected for two years, between 2007 and 2008, during the Earth-to-satellite Syracuse 3 propagation experiment. The originality of the experimental set-up is the use of a 44-GHz uplink at a low elevation angle of 17°. The statistical analysis of the attenuation levels has shown the validity of ITU predictions for such a configuration (within interannual variability). As far as frequency scaling is concerned, the specific ratio for rain attenuation given by ITU recommendations cannot be used directly since, at 44 GHz, gas and cloud contributions cannot be neglected. A model in which these effects are separated has been tested and found to be in good agreement with the empirical instantaneous frequency scaling ratio. As to fade duration statistics, it has been found that the ITU model does not fit correctly our experimental data, especially for short fade durations, whereas the Cheffena–Amaya model shows a better agreement.

For real-time fade mitigation, the ARIMA-GARCH attenuation prediction model developed on the basis of Olympus 20-GHz data has been validated on the Syracuse 3 20-GHz data, indicating that this model can be considered to be general and not specific to a given link. The comparison of the model parameters shows that they are not strongly sensitive to link geometry. The prediction model was tested against other existing models over a whole year of data and performance assessment confirmed that it outperforms the other models significantly in terms of link availability. Finally, the ARIMA-GARCH model has been combined with a Ka-band to Q-band frequency scaling method in order to predict the uplink channel propagation conditions from downlink measurements. Although the performance of this model would make its implementation advantageous for system designers, it was found that frequency scaling causes a significant increase in the prediction error. Its contribution to the total error is indeed greater than the one due to the downlink prediction. This shows that there is a need for improving the accuracy of the frequency scaling factor, or that the prediction method should be applied directly to the overall point-to-point attenuation, i.e. to the sum of the uplink and downlink attenuations.

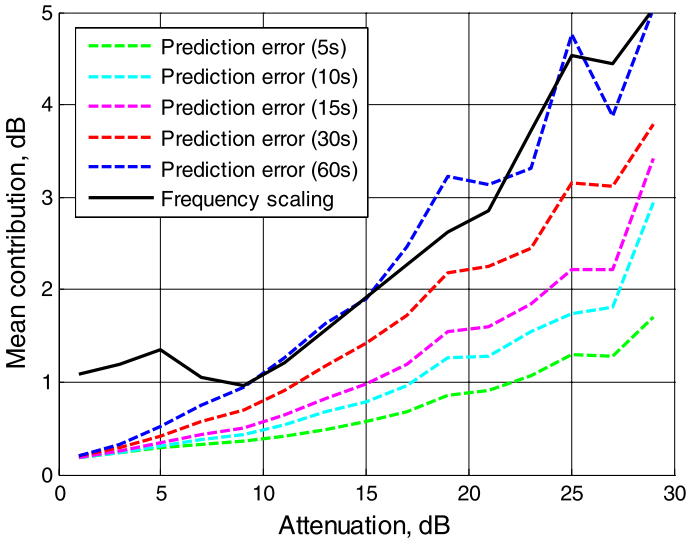

Fig. 10. Contributions to the total prediction error of the frequency scaling method and of ARIMA-GARCH for various forecast intervals versus 44-GHz total attenuation.

References

[1] M. Cheffena, C. Amaya, Prediction model of fade duration statistics for satellite links between 10–50 GHz, IEEE Antennas and Wireless Propagation Letters 7 (2008).
[2] L. de Montera, et al., Short-term prediction of rain attenuation level and volatility in Earth-to-satellite links at EHF band, Nonlin. Process. Geophys. 15 (4) (2008) 631–643.
[3] T. Marsault, et al., EHF propagation experiment with Syracuse 3 satellite: First results, in: 2nd European Conference on Antennas and Propagation (EuCAP), 2007.
[4] J.-Y. Delahaye, et al., A dual-beam spectropluviometer concept, J. Hydrol. 328 (2006) 110–120.
[5] C. Mallet, J. Lavergnat, Beacon calibration with a multifrequency radiometer, Radio Sci. 27 (5) (1992) 661–680.
[6] L. Barthes, et al., Neural network model for atmospheric attenuation retrieval between 20 and 50 GHz by means of dual-frequency microwave radiometers, Radio Sci. 38 (5) (2003) 1082.
[7] ITU-R (618-9, 676-6, 840-3), International Telecommunication Union Radiocommunication Bureau, Geneva, 2007.
[8] J.C. Gibbins, Improved algorithms for the determination of specific attenuation at sea level by dry air and water vapor, in the frequency range 1–350 GHz, Radio Sci. 21 (6) (1986) 949–954.
[9] H.J. Liebe, MPM – An atmospheric millimeter-wave propagation model, Int. J. Infr. Mill. Waves 10 (1989) 631–650.
[10] ITU-R P1623-1, International Telecommunication Union Radiocommunication Bureau, Geneva, 2003–2005.
[11] P. Golé, et al., Les résultats de l'expérience OLYMPUS France Telecom FTR&D, technical report NT/CETP/001, 1994.
[12] OPEX, Second Workshop of the OLYMPUS Propagation Experimenters, vol. 1: Reference Book on Attenuation Measurement and Prediction, Noordwijk, 8–10 Nov. 1994.
[13] S. Lovejoy, D. Schertzer, Turbulence, rain drops and the $l^{1/2}$ number density law, New J. Phys. 10 (2008) 075017.
[14] A.M. Bolea-Alamañac, et al., Implementation of short-term prediction models in fade mitigation techniques control loops, in: COST 272/280 Workshop, ESA/ESTEC, Noordwijk, The Netherlands, 2003, PM5-067.
[15] L. Castanet, et al., Channel modelling based on N-state Markov chains for SatCom systems simulation, in: ICAP 2003, Exeter, UK, 2003, pp. 119–122.
[16] M.M.J.L. Van de Kamp, Short-term prediction of rain attenuation using two samples, Electron. Lett. 38 (23) (2002) 1476–1477.
[17] R.M. Manning, A unified statistical rain attenuation model for communication link fade predictions and optimal stochastic fade control design using a location dependent rain statistic database, Int. J. Satellite Commun. 8 (1990) 11–30.
[18] R.M. Manning, A statistical rain attenuation prediction model with application to the Advanced Communication Technology Satellite Project, part III: A stochastic rain fade control algorithm for satellite link power via nonlinear Markov filtering theory, NASA, 1991, TM-100243.
[19] A.P. Chambers, L.E. Otung, Neural network approach to short-term fade prediction on satellite links, Electron. Lett. 41 (23) (2005) 1290–1292.
[20] B. Grémont, et al., Comparative analysis and performance of two predictive fade detection schemes for Ka-band fade countermeasures, IEEE J. Select. Areas Commun. 17 (2) (1999) 180–192.